Theoretical study of the time-dependent phenomenon of photon-assisted tunneling through a charged quantum dot

2009 J. Phys.: Condens. Matter 21 064230

(http://iopscience.iop.org/0953-8984/21/6/064230)

IOP Publishing Journal of Physics: Condensed Matter

J. Phys.: Condens. Matter **21** (2009) 064230 (5pp) doi:10.1088/0953-8984/21/6/064230

Theoretical study of the time-dependent phenomenon of photon-assisted tunneling through a charged quantum dot

Masakazu Muraguchi[1,3], **Kenji Shiraishi**[1], **Takuma Okunishi**[2] and **Kyozaburo Takeda**[2]

[1] Graduate School of Pure and Applied Sciences, University of Tsukuba, Tennodai, Tsukuba, Japan

[2] Department of Electrical Engineering and Bioscience, Waseda University, Shinjyuku, Tokyo, Japan

E-mail: muraguchi@comas.frsc.tsukuba.ac.jp

Received 20 July 2008, in final form 11 September 2008
Published 20 January 2009
Online at stacks.iop.org/JPhysCM/21/064230

Abstract

We have studied numerically the time-dependent photon-assisted tunneling (TD-PAT) process for electrons confined in quantum dots (QDs) by employing the finite difference method under the scheme of the TD-density functional theory (DFT). We have found the *quasi*-dark state (*quasi*-DS), where the injected electron remains in the QD. By varying the barrier thickness, we have calculated the TD profile of the electron density in a QD, and found the optimal geometry of the lozenge QD. We have also discussed how the charged QD modulates the PAT process.

(Some figures in this article are in colour only in the electronic version)

1. Introduction

The precise control of electronic states in quantum dots (QDs) has attracted much interest for applications involving quantum effect devices. Of the various techniques, employing a time-dependent (TD) field, such as an ac electric or electromagnetic field, is regarded as being one of the most promising techniques for controlling electrons in QDs [1–6]. However, under a TD field, the electron wavefunction in the QD significantly changes its shape within an extremely short time [7, 8]. Thus, an accurate knowledge of the TD electron wavefunction is required.

In our previous work, we have theoretically studied the dynamic properties of photon-assisted tunneling (PAT) in a two-dimensional (2D) but uncharged QD, focusing on the lifetimes of individual resonant states. We revealed that the total lifetime for an electron under PAT is determined by the superposition of the lifetimes of the individual resonant states [9]. We further demonstrated that an appropriate choice of the resonant transition(s) enabled us to tune the electron lifetime artificially, and succeeded in creating a 'dark state', where the PAT electron hardly tunnels via the QD but remains in the QD.

The lifetime of the PAT electron is a crucial parameter for controlling the ultra-fast TD phenomenon in the QD. In the present work, we study the controllability of the PAT phenomena via the 'dark state', focusing on this lifetime. First, we considered an uncharged lozenge shaped QD, and determined the optimal barrier thickness for formation of the dark state. We further extended our study to determine how the charging of the QD modulates the PAT process.

2. Model and method

2.1. Model

We considered the lozenge shaped QD system shown in figure 1, in which we expect the momentum components of the electron wavepacket to convert the direction of propagation to a perpendicular one. Both sides of the QD are connected to leads for electron propagation (figure 1). We suppose the QD to be an AlGaAs QD fabricated on a GaAs substrate system, where it has a potential barrier height of 0.3 eV and a thickness of $d = 2.5$ nm, whereas the leads are surrounded by a potential

[3] Present address: Center for Interdisciplinary Research, Tohoku University, 6-3 Aramaki aza-Aoba, Aoba-ku, Sendai 980-8578, Japan.

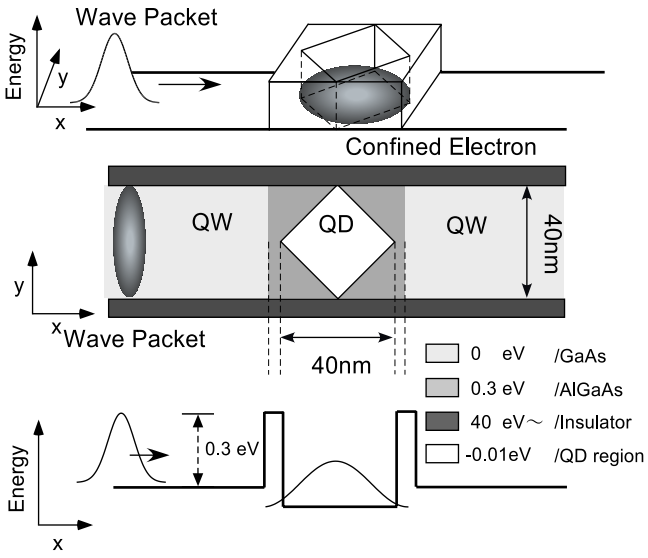

Figure 1. Illustration of the present lozenge shaped QD system, where both sides of the QD are connected to leads for electron propagation. An electron wavepacket is injected into the QD from the left lead. We set the diameter of the QD to be 40 nm. Note that the bottom of the potential of the QD is 10 meV below that in the uncharged condition. Other geometrical parameters and potential profiles are indicated in the figure.

wall with infinite barrier height. We also assumed that the electrons are confined in two dimensions but that the induced Coulomb potential extends to three dimensions. We made the further simplification that the barrier shape of the present system is a well-defined hard wall. We also set the barrier height of the QD to be 10 meV lower than the leads when the QD is uncharged. We injected an electron wavepacket from the left lead to the charged/uncharged 2D QD in the photon-electric field.

2.2. Calculational method

We employed time-dependent density functional theory (DFT) to study the time evolution of the wavefunctions within the framework of the local spin density approximation including the self-interaction correction (LSDA + SIC). Thus, we used the following equations;

$$h_{\mathrm{ks}}(\mathbf{r},t) = -\frac{\hbar^2}{2m^*}\nabla^2 + v^{\sigma}_{\mathrm{eff}}(\mathbf{r}), \tag{1}$$

$$v_{\mathrm{eff}}(\mathbf{r}) = V_{\mathrm{ee}}(\mathbf{r},t) + V^{\sigma}_{\mathrm{xc}}(\mathbf{r},t) + V_{\mathrm{ext}}(\mathbf{r},t), \tag{2}$$

$$V^{\sigma}_{\mathrm{xc}} = \frac{\delta E_{\mathrm{xc}}[\rho^{\alpha},\rho^{\beta}]}{\delta\rho^{\sigma}(\mathbf{r})} - \int \frac{\rho^{\sigma}(\mathbf{r}')\,\mathrm{d}\mathbf{r}'}{|\mathbf{r}-\mathbf{r}'|} - \frac{\delta E_{\mathrm{xc}}[\rho^{\sigma},0]}{\delta\rho^{\sigma}(\mathbf{r})}, \tag{3}$$

where $\mathbf{r}$ is the position vector, σ, the spin coordinate and ρ, the density of the Kohn–Sham (KS) orbital [10]. The external potential $V_{\mathrm{ext}}(\mathbf{r},t)$ consists of two terms:

$$V_{\mathrm{ext}}(\mathbf{r},t) = V_{\mathrm{ph}}(\mathbf{r},t) + V_{\mathrm{stat}}(\mathbf{r}), \tag{4}$$

where V_{stat} represents the static potential field, which determines the QD and semi-infinite leads. The second term V_{ph} represents the electric field of the photon used to irradiate the QD. Note that the present V_{stat} allows us to employ the dipole approximation for the electron–photon interaction semi-classically because we fixed the diameter of the present QD to be 40 nm. The resulting energy differences between the single-electron eigenstates are of the order of several tens to hundreds of meV. Thus, photons having terahertz-order frequencies are required for the present PAT, and the corresponding wavelengths of the photons are larger than the present QD area. Therefore the $V_{\mathrm{ph}}(\mathbf{r},t)$ is approximately expressed by

$$V_{\mathrm{ph}}(\mathbf{r},t) = E_0\mathbf{r}\sin(\omega t), \tag{5}$$

where E_0 and ω are the intensity and frequency of the photon-electric field, respectively. It is also reasonable that the photons interact with electrons in the QD area only, because the present GaAs QD barrier significantly reduces the degree of penetration of the wavefunction into the lozenge barrier region. The symbol V_{xc} represents the exchange–correlation potential with the self-interaction correction [11]. In order to solve the TD-KS equation, we employ a finite difference technique using a real-space mesh. Details have been reported in our previous works [7–9].

We study the resonant tunneling through the individual resonant states. For this, the injected wavepacket should be spatially extended. Therefore, the energy of the wavepacket is defined by its central momentum. Thus, we inject an electron from the left lead into the QD as a wavepacket with the following Gaussian form:

$$\psi_{\mathrm{in}}(x,y,0) = \frac{1}{\pi^{1/4}\sqrt{d}}\exp\left[-\frac{(x-x_0)^2}{2d^2}\right] \times \left[\mathrm{i}\frac{p_x}{\hbar}(x-x_0)\right]\cos\frac{\pi}{a}(y-y_0). \tag{6}$$

Here, we modify the plane wave representing the electron propagation in the x-direction with momentum p_x, whereas the cosinusoidal standing wave is assumed to expand in the y-direction. We also set the electron wavepacket to be initially placed at $(x_0, y_0) = (-1280, 0)$ nm with a real-space Gaussian distribution with $d = 320$ nm. The symbol a represents the width of the leads, the value of which is 40 nm.

To obtain a precise picture of the tunneling process, we employ projection analysis, where we project the propagating wavefunction $\psi(x,y,t)$ into the resonant states of the QD $\phi^0_n(x,y)$ defined as follows;

$$P_n(t) = \int_{\mathrm{QD}} \psi(x,y,t)\phi^0_n(x,y)\,\mathrm{d}x\,\mathrm{d}y \qquad n = 1,\ldots,N, \tag{7}$$

where we use the nth resonant state $\phi^0_n(x,y)$, which has been numerically obtained by solving the time-independent Schrödinger equation in real space. Resonant states up to $N = 24$ are taken into account.

2.3. Symmetry of the system

The calculated one-electron eigenstates for the lozenge shaped QD are given in figure 2, where all the eigenstates are classified

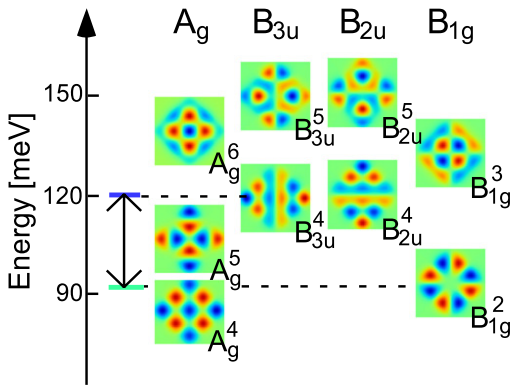

Figure 2. Calculated eigenstates for an electron confined in a lozenge shaped QD. The eigenstates are assigned by their irreducible representations and sequential numbers in the order of their energy.

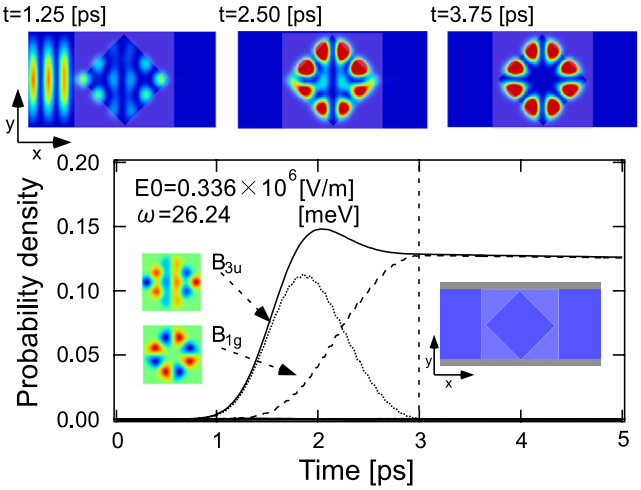

Figure 3. Time evolution of the total electronic density for an injected electron (solid line) and its projection on to the eigenstates of the QD (dotted lines) under photon irradiation ($E_0 = 1.175 \times 10^5$ V m^{-1}, $\omega = 26.24$ meV) is cut off at $t = 3.0$ ps when the partial probability density of B^2_{1g} reaches its first maximum. The insets represent snapshots of the eigenstates and the potential profiles of the lozenge shaped QD. Several snapshots of the probability density are also given.

in terms of the irreducible representation of the point group symmetry of D_{2h}. This is because the connection of the leads lowers the symmetry of the present QD system from D_{4h} to D_{2h}. Thus, the resulting resonant states have orbital symmetries of A_g, B_{3u}, B_{1g}, and B_{2u}. The sequential number found in the individual superscripts indicates the order of the energy.

When we inject an electron as a nodeless wavepacket having an even symmetry perpendicular to the direction of propagation (y-direction), the electron can only transmit through the resonant states A_g or B_{3u}. The geometrical symmetry forbids an electron to tunnel through the resonant states B_{2u} or B_{1g}.

3. Controlling the PAT process in the QD

3.1. Quasi-dark state

We inject an electron (wavepacket) into the resonant state B^4_{3u} (figure 2), whereas the QD is irradiated by photons whose electric field is polarized in the y-direction, having an energy of 26.24 meV. Because this energy coincides with the energy difference between the resonant states B^4_{3u} and B^2_{1g}, the injected electron transits into the resonant state B^2_{1g} during electron tunneling, and the PAT process occurs.

The total (solid line) and the partial electronic densities (broken lines) and several snapshots are shown in figure 3. One can find the characteristic PAT process, where the electronic state of the tunneling electron changes from the resonant state B^4_{3u} to B^2_{1g} at $t \simeq 3$ ps. The transited resonant state B^2_{1g} has an odd symmetry in the y-direction, whereas the potential barrier surrounding the QD has an even symmetry. We switched off the photon irradiation to prevent Rabi oscillations at $t = 3$ ps. Thus, the tunneling electron hardly flows out, and the resulting electron remains inside the QD. We previously called this state a '*quasi*-dark state (*quasi*-DS)' [9].

3.2. PAT process in a QD with a thin barrier

We reduced the width of the lozenge barrier to increase the inflow of injected electrons into the QD and enhance the *quasi*-

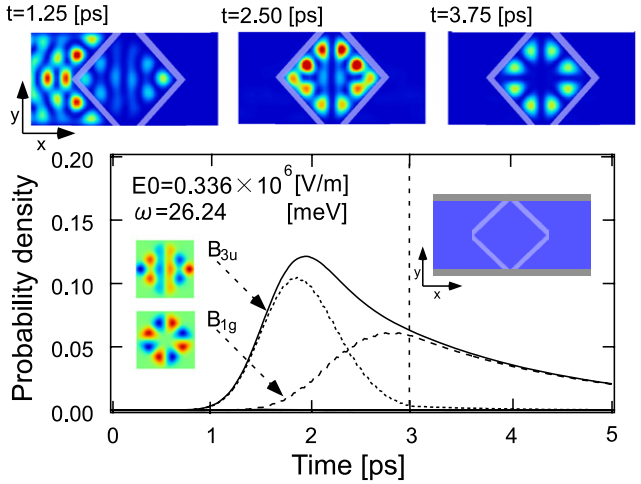

Figure 4. Time evolution of the total electronic density for an injected electron (solid line) and the constituent eigenstates P_n (dotted lines) in a QD surrounded by a thin barrier. The photon-electric field is polarized in the y-direction ($E_0 = 0.336 \times 10^6$ V m^{-1}, $\omega = 26.24$ meV) and is switched off at $t = 3.0$ ps. The insets show snapshots of the eigenstates and the potential profiles. Several snapshots of the probability density are also given.

DS. The TD profile of the electron density in the QD, in which the barrier thickness has been reduced from 20.0 to 2.5 nm is shown in figure 4. Similar to figure 3, one can find the analogous TD-PAT process in this thin-barrier QD.

We, then, switched off the photon irradiation at $t = 3$ ps in order to produce the *quasi*-DS. However, we were unable to find the characteristic *quasi*-DS, but there was a significant reduction in the electronic state B^2_{1g}. The thin barrier serves to

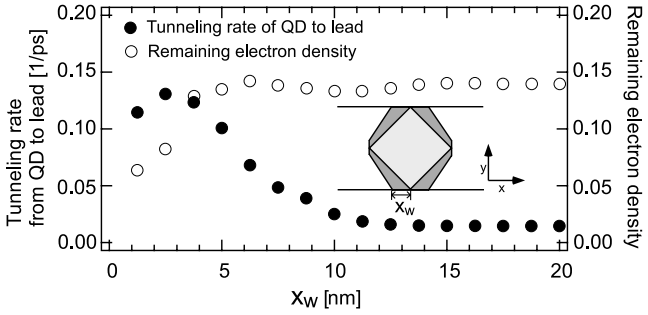

Figure 5. The electron density remaining in the QD (right axis) and the tunneling rate from the QD to the lead (left axis) for various potential thicknesses. The remaining electron density remains constant once the barrier thickness has reached 2.5 nm, while the tunneling rate from the QD increases as the barrier thickness decreases. The definition of the barrier thickness X_w is shown in the inset.

increase the outflow of tunneling electrons from the QD. This is because the outflow of electrons from the QD is determined by the electron density distribution rather than by the symmetry of the wavefunction itself. The electronic subbands in the left lead have both even and odd symmetries in the y-direction. Consequently, the resulting *quasi*-DS should be shortened in the thin-barrier QD.

3.3. Optimal geometry of QDs for controlling electron propagation

In order to obtain the optimal geometry of the QD, we studied the changes in electron propagation when varying the barrier thickness. We define the barrier thickness as shown in the inset of figure 5, where we vary the thickness from 2.5 to 20.0 nm.

First, we discuss the tunneling rate from the QD into the lead when the photon irradiation is switched off (t = 3.0 ps). Figure 5 (filled circle) reveals that the tunneling rate remains constant as the barrier thickness is decreased, but increases exponentially when the barrier thickness is less than 10 nm.

We next focus on the electron density remaining in the QD at t = 3.0 ps. Figure 5 (open circle) shows that this value hardly changes with barrier thickness. This feature is due to the geometrical characteristics between the injected electron (wavepacket) and the QD. In the present calculation, the injected electron has a high density around the propagating axis, whereas in the present QD the barrier thickness (2.5 nm) of the central gate is conserved. This geometry ensures that the change in barrier thickness does not alter the tunneling process into the QD. We therefore conclude that the well established *quasi*-DS is expected to arise when the QD has a barrier thickness larger than 10 nm.[4]

[4] Note that both the tunneling rate (from the QD to the lead) and the injection probability (the remaining electron density) significantly decrease around the condition X_w = 2.5 nm. This is because the barrier thickness is too small to retain the electron within the QD.

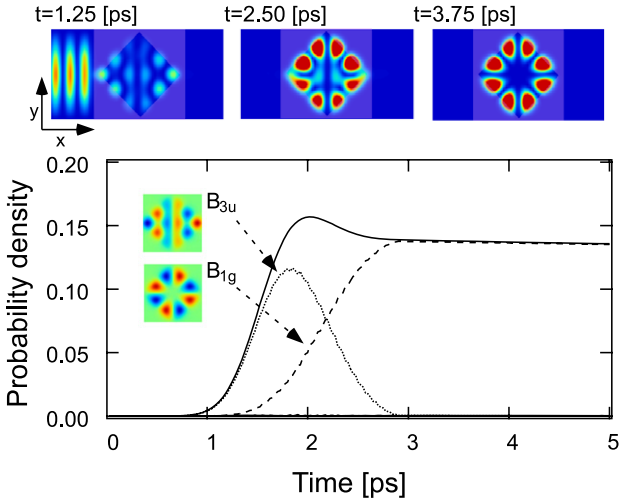

Figure 6. The time evolution of the total electronic density for the injected electron (solid line) and the constituent eigenstates P_n (dotted lines) in the charged QD. The initial energy of the electron wavepacket is 140 meV. The photon-electric field is polarized in the y-direction and is switched off at t = 3.0 ps ($E_0 = 1.175 \times 10^5$ V m^{-1}, ω = 26.24 meV). The insets show the spatial distributions of the eigenstates. Several snapshots of the probability density are also given.

4. Controlling a PAT process in a charged QD

4.1. PAT process in a charged QD

We also studied how charging of the QD changes the characteristics of the *quasi*-DS. We confined an electron in the ground state of the QD, supposing the total spin multiplicity of the present system to be a singlet. Similar to the case of the uncharged QD, an electron wavepacket is injected into the resonant state B^4_{3u} (figure 6). Note that the resonant state B^4_{3u} is energetically about 20 meV higher than that in the uncharged QD due to the charge on the electron. Figure 6 shows the TD profile of the electron density in the QD. It reveals that the crossing time between the resonant states B^4_{3u} and B^2_{1g} is at 2.3 ps, which is almost equal to that found in the uncharged state as shown in figure 3. Here, the electron transits to the B^2_{1g} state at t = 3.0 ps. As a result, the *quasi*-DS appears if the photon irradiation is switched off at that time. Thus, one can find a TD-PAT process similar to that found in the uncharged QD.

4.2. Tunneling probability for charged and uncharged QDs

In order to clarify the effect of the charged electron more precisely, we compare the tunneling probability in the charged QD with that in the uncharged one without photon irradiation (figure 7). An electron wavepacket is injected into the QD by varying the initial kinetic energy. We calculate the tunneling probability into the right lead when sufficient time has passed. We find that the charged electron shifts the peaks uniformly towards higher energies by about 20 meV, whereas the peaks conserve their individual heights. This is because we place an electron in the ground state, which produces a uniform

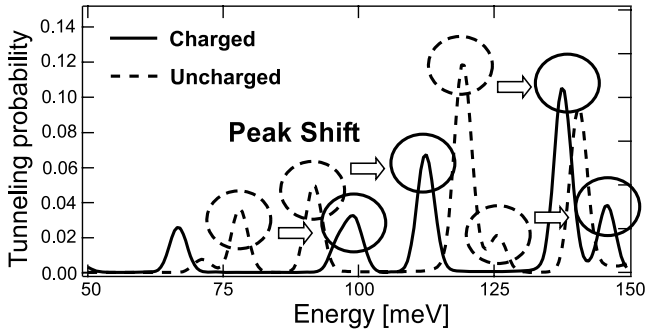

Figure 7. The tunneling probability of an electron wavepacket through a charged and uncharged QD. The solid and dashed lines show the charged and uncharged conditions, respectively. The values are obtained from the probability density in the right lead by varying the kinetic energy of the injected wavepacket with no photon irradiation.

distribution in the QD. Consequently, the charged electron plays the simple role of a static potential in the tunneling process. Thus, the characteristic TD features in the PAT process should be conserved between charged (figure 3) and uncharged QDs (figure 7).

5. Summary

We employed a TD-DFT approach and used a finite difference method to study a TD-PAT process for electrons confined in a QD. We revealed that the symmetry of the wavefunction and the geometry of the QD potential determine the process by which electrons tunnel into the QD, whereas the barrier thickness is crucial in determining the electron outflow from the QD. By varying the barrier thickness, we calculated the TD profile of the electron density in the QD. We found that the present lozenge shaped QD with a thickness greater 10 nm can give rise to a well-defined *quasi*-DS. We also clarified how the PAT process can be modulated in the charged QD. The charged electron shifts the resonant-tunneling peaks uniformly towards higher energies, whereas the heights of individual peaks are conserved. This is because we placed the electron in the ground state, which produces a uniform distribution in the QD. Consequently, the charged electron plays the simple role of a static potential in the tunneling process. Thus, the characteristic TD features in the PAT process should be the same both in charged and uncharged QDs.

Acknowledgments

This work was supported by Grant-in-Aid for Science Researches Nos 18063003 and 20760019 from the Ministry of Education, Science, Sports, and Culture, Japan. Numerical calculations in the present study were performed by the supercomputer centers of the Institute of Molecular Science, and the Institute for Solid State Physics, University of Tokyo.

References

[1] Sollner T C L G, Brown E R, Goodhue W D and Le H Q 1987 *Appl. Phys. Lett.* **50** 332
[2] Besombes L, Baumberg J J and Motohisa J 2003 *Phys. Lett.* **90** 257402
[3] Bonadeo N H, Erland J, Gammon D, Park D, Katzer D S and Steel D G 1998 *Science* **20** 1473
[4] Chitta V A, de Bekker R E M, Maan J C, Hawksworth S J, Chamberlain J M, Henini M and Hill G 1992 *Surf. Sci.* **263** 227
[5] Bulgakov E N and Sadreev A F 1996 *J. Phys.: Condens. Matter* **6** 8869
[6] Jauho A P 1990 *Phys. Rev.* B **41** 12327
[7] Koiso T, Muraguchi M and Takeda K 2005 *Japan. J. Appl. Phys.* **44** 4252
[8] Okunishi T, Muraguchi M and Takeda K 2007 *Phys. Rev.* B **75** 245314
[9] Muraguchi M and Takeda K 2007 *Japan. J. Appl. Phys.* **46** 1224
[10] Runge E and Gross E K U 1984 *Phys. Rev. Lett.* **52** 997
[11] Kohn W and Sham L J 1965 *Phys. Rev.* **140** 1133